Influence of Ho2O3 on Optimizing Nanostructured Ln2Te6O15 Anti-Glass Phases to Attain Transparent TeO2-Based Glass-Ceramics for Mid-IR Photonic Applications

GUPTA, Gaurav <http://orcid.org/0000-0002-2948-6740>, BYSAKH, Sandip, BALAJI, Sathravada, KHAN, Sultan, BISWAS, Kaushik, ALLU, Amarnath R and ANNAPURNA, Kalyandurg <http://orcid.org/0000-0002-7719-7644>

Published version

GUPTA, Gaurav, BYSAKH, Sandip, BALAJI, Sathravada, KHAN, Sultan, BISWAS, Kaushik, ALLU, Amarnath R and ANNAPURNA, Kalyandurg (2020). Influence of Ho2O3 on Optimizing Nanostructured Ln2Te6O15 Anti-Glass Phases to Attain Transparent TeO2-Based Glass-Ceramics for Mid-IR Photonic Applications. Advanced Engineering Materials, 22 (5), p. 1901357.

Supporting Information

Influence of Ho_2O_3 on Optimizing Nanostructured $Ln_2Te_6O_{15}$ *anti*-glass Phases to Attain Transparent TeO_2-based Glass-ceramics for Mid-IR Photonic Applications

Gaurav Gupta[a], Sandip Bysakh[b], Sathravada Balaji[a], Sultan Khan[a], Kaushik Biswas[a], Amarnath R. Allu[a], Kalyandurg Annapurna[a]*

[a]Glass Division, CSIR-Central Glass and Ceramic Research Institute 196, Raja S. C. Mullick Road, Kolkata 700 032, India

[b]Electron Microscopy Section Materials Characterization Division, CSIR-Central Glass and Ceramic Research Institute 196, Raja S. C. Mullick Road, Kolkata 700 032, India

*Corresponding author:

Email: annapurnak@cgcri.res.in

Fax: +91-33-24730957

Phone: +91-33-24733496

Contents:

S1. Glass synthesis and characterizations

For the study of present series of glass, authors have considered a multi-component tellurite glass doped with various lanthanide species which have the composition as, 80 TeO_2 – 10 TiO_2 – 5 Gd_2O_3 – (5 – *x*) La_2O_3 – *x* Ho_2O_3 (in mol %) where, *x* = 0, 1, 2. The sample without Ho_2O_3 has been labelled as TTLG further and the samples with 1 and 2 mol% of Ho_2O_3 doping have been labelled as TTLGH1 and TTLGH2 respectively. These series of glass has prepared at the melting temperature of 900 °C, with the utilization of the pure Platinum crucible. In the 1 h melting-schedule, homogeneous glass samples have achieved after an intermittent stirring using pure Platinum wire. Thermal stress-free glass blocks have accomplished by the introduction of annealing at 350 °C of temperature (i.e., less than T_g). The series of annealed glass blocks have cut and finely polished to a plate of typical thickness of 2 mm, for further experimentation.

The refractive indices of all the samples were measured using prism coupler (Model: Metricon M 2010; Metricon,USA) equipped with 5 different wavelengths (473, 532,632.8, 1064, 1552 nm). The DSC curve were recorded using DTA/DSC thermal analyzer (Model: STA449 F3; NETZSCH GmbH, Germany) under N2atmo-sphere with heatin[1]g rate of 10 °C/min from room temperature to 900°C. DSC experiments were carried out using standard DSC platinum crucibles on glass powders weighing about 30-40 mg each with particle size <100 μm.

S2. Refractive indices and dispersion relationships

Dispersion relationship of the TTLG glasses has been measured via refractive index. The prism coupler method has been adopted to measure the refractive index of the glass and transparent glass-ceramics. The measured refractive indices are fitted with the Sellmeier dispersion equation as described in our earlier work.[1]

The measured refractive index of the transparent glass and glass-ceramics reveal that with the increase of ceramization duration its refractive index increases considerably. The increase in the refractive indices upon ceramization duration has been associated to the size of phase separated domains. According to Chenu *et. al.* [2], the refractive indices of the material can be

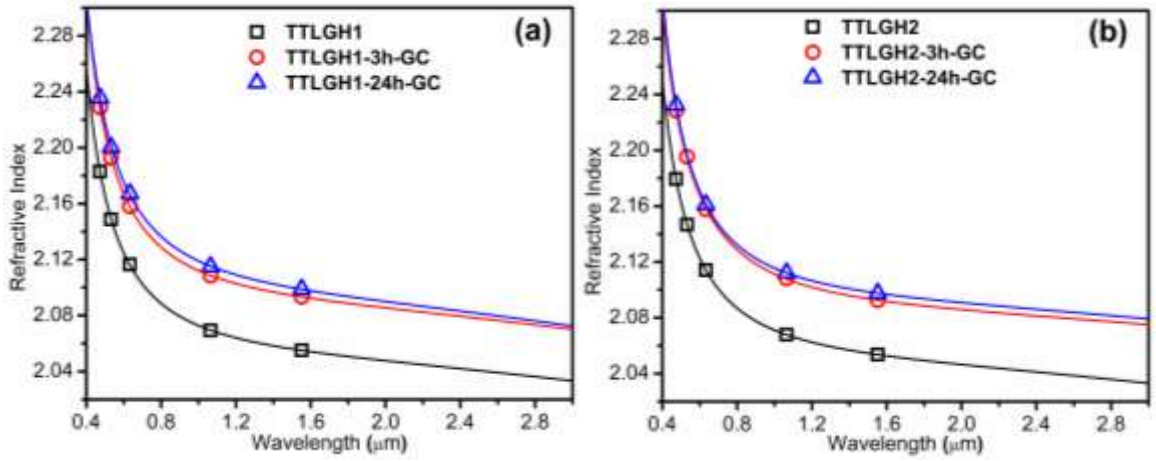

Figure S-I: The measured refractive index (*n*) with accuracy of ±0.0002 has fitted with Sellmeier dispersion equation for (a) TTLGH1 and (b) TTLGH2 based

correlated with their maximum attainable transparency by the relation $T_{max}=[2n/(n^2+1)]\times 100$. The increase of refractive indices of the glass-ceramics has effectively reduced its transparency. This is supporting the trend observed in transmission spectra of the present series of glass-ceramics.

S3. TEM sample preparation and STEM-EDX elemental map of glass-ceramics

The nanostructures of glass and glass-ceramic samples were investigated by using a transmission electron microscope (TEM; FEI Model Tecnai G2 30ST; Hillsboro, OR, USA). The glass samples for TEM measurement were prepared by crushing the glass powder in methanol

medium by using a mortar and pestle into a fine form and one drop of the dispersion was deposited on the carbon film coated copper grid. In order to obtain large electron transparent region of interest for the glass-ceramic samples, thin foil sample preparation technique using Ar^+-ion-milling has been adopted. Due to the brittle nature of TeO_2 based glass-ceramic sample, the normal method of grinding and polishing of 3 mm punched discs towards the thin foil sample preparation with few tens of nanometer thickness was unfeasible. Thus to achieve electron transparent glass-ceramics thin foil with significant area novel technique has been implemented. A solid stainless steel rod of 2.6 mm diameter has been sliced axially along a diameter of the rod cross-section by using a diamond saw (Buehler Low Speed Saw, Buehler Inc., USA) with double blades to make a slit of about 1 mm width within which the sliced glass-ceramic material of appropriate dimension has been fixed using Gatan G-1 epoxy. This rod holding the glass-ceramic piece into its slot has been inserted and glued with Gatan G-1 epoxy inside a hollow stainless steel tube having inner diameter of 2.7 mm and outer diameter of 3 mm. The whole glued arrangement was cured at a temperature of 125 ^oC for 10 minutes. In consequence of curing reaction the glass-ceramic sample was securely fixed. This glued cylinder containing the glass-ceramic at the centre is sectioned by the low speed diamond saw to obtain slices of about 250 μm thickness. Each slice was mounted on stainless steel stub to be grinded and polished on both sides gradually on 40, 15 and 5 μm emery paper down to a thickness of 100 μm by using Gatan Disc Grinder (Gatan Inc., USA) having micrometer scale for thickness monitoring. This polished disc was further grinded and polished at the centre by using 5 micron diamond paste and 0.05 micron Alumina suspension in a Gatan Dimple Grinder (GATAN Inc., USA) to retain 20 μm thicknesses at the centre of this sectioned disc where a slice the glass-ceramic sample is located.

This dimple-polished 3 mm diameter TEM specimen was then Argon ion-milled on both top and

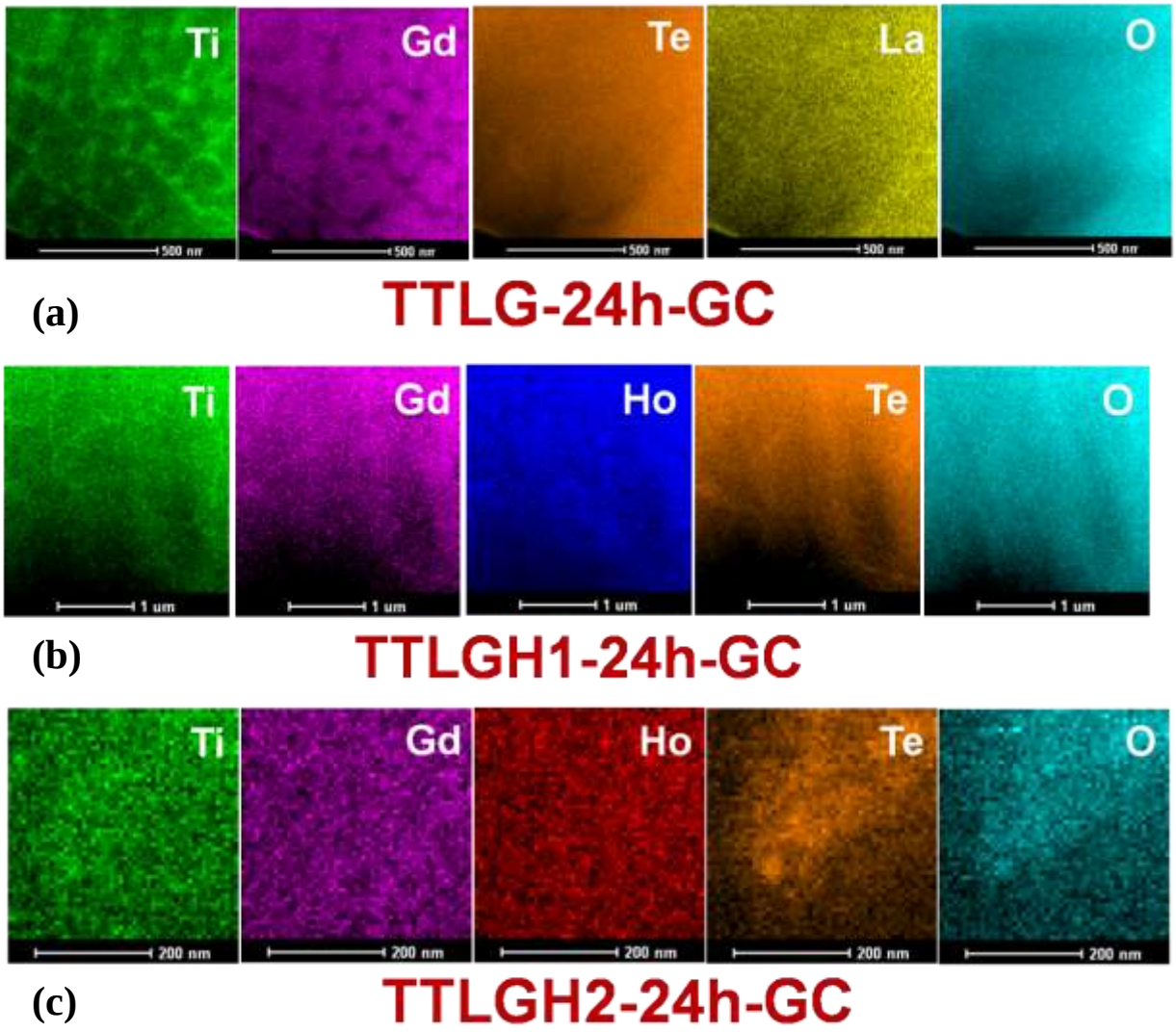

Figure S-II: The elements in the glass-ceramics EDX point mapping of (a) TTLG-24h-GC, (b) TTLGH1-24h-GC and (c) TTLGH2-24h-GC samples.

bottom side at 2.5 kV and 4 ^{o} angles of Ar^{+} ion-beam incidence and double-sector ion milling, using GATAN Model 691 Precision Ion-Polishing System (PIPS) to obtain perforations where electron transparent areas suitable for TEM imaging are formed. Finally, a carbon coating of 5 nm thickness was deposited on this perforated sample by using GATAN Precision Etching and

Coating System (PECS), to avoid the specimen charging during TEM observation. The distribution of the constituent elements within the glass-ceramic sample was investigated using a Tecnai G^2 30ST TEM operating at 300 kV and equipped with a LaB_6 thermionic electron source. Scanning transmission electron microscopy–high angle annular dark field (STEM-HAADF) images were acquired with a camera length of 120 cm and a probe size of 5 nm. The contrast of these dark-field images is linked to the square of atomic number (*Z*) of the constituent elements and thus allows one to obtain a chemical contrast. Attempts were also made to obtain Elemental distribution maps by employing the STEM-EDX spectrum imaging technique using an EDX Spectrometer (EDAX Inc., USA) detector and a probe size of 5 nm in order to have better insight into the phase separation in the glass-ceramic system. Supplementary information S-II (a), (b), and (c) have been depicting the STEM-EDX elemental maps of TTLG-24h-GC, TTLGH1-24h-GC and TTLGH2-24h-GC respectively. The detailed analysis of the STEM-EDX patterns of glass-ceramics has been given in the main text.

S4. SAED patterns of glass-ceramics

The SAED pattern of TTLG-24h-GC and TTLGH2-24h-GC samples are presented in the supplementary information S-VI (a) and (b) respectively. In case of the glass-ceramics TTLG-24h-GC, the superstructure patterns are not observed. On the contrary, the ring patterns were

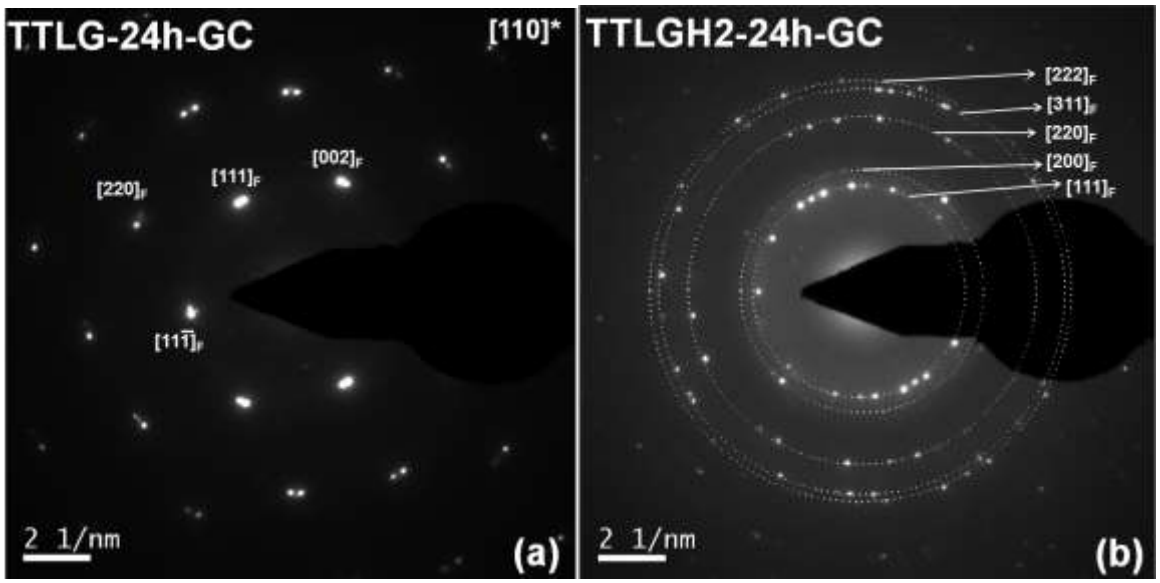

Figure S-III: SAED pattern of (a) TTLG-24h-GC and (b) TTLGH2-24h-GC samples

observed in case of TTLGH2-24h-GC sample. These patterns were discussed vehemently in the result and discussion part of the main text.

S5. Local structural evolution of *titanium tellurite* glass modified with lanthanides

As mentioned in the main text, the measured Raman spectra of the glass series has been modified

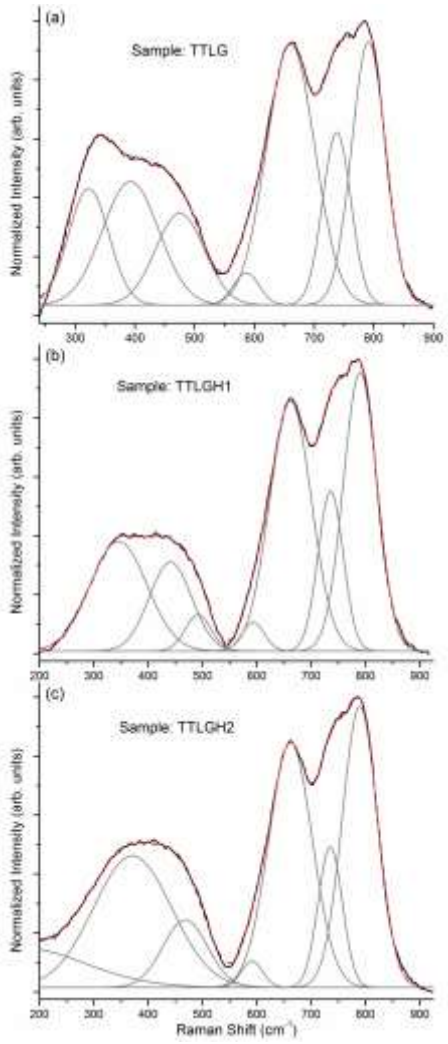

Figure S-IV: The deconvoluted Raman spectra of (a) TTLG, (b) TTLGH1 and (c) TTLGH2 glass samples (solid black line is the modified and normalized spectra and dashed red line is the sum of deconvoluted spectra).

and normalized. Barney *et. al*. have deconvoluted the Raman spectra of pure amorphous TeO_2 glass for 550 – 900 cm^{-1} region.[3] For the present series of TeO_2-based glass, the scheme of Barney *et al*. has been adopted. The deconvoluted Raman spectra of TTLG, TTLGH1 and

TTLGH2 glass have been depicted in the Supplementary information S-IV (a), (b), and (c)

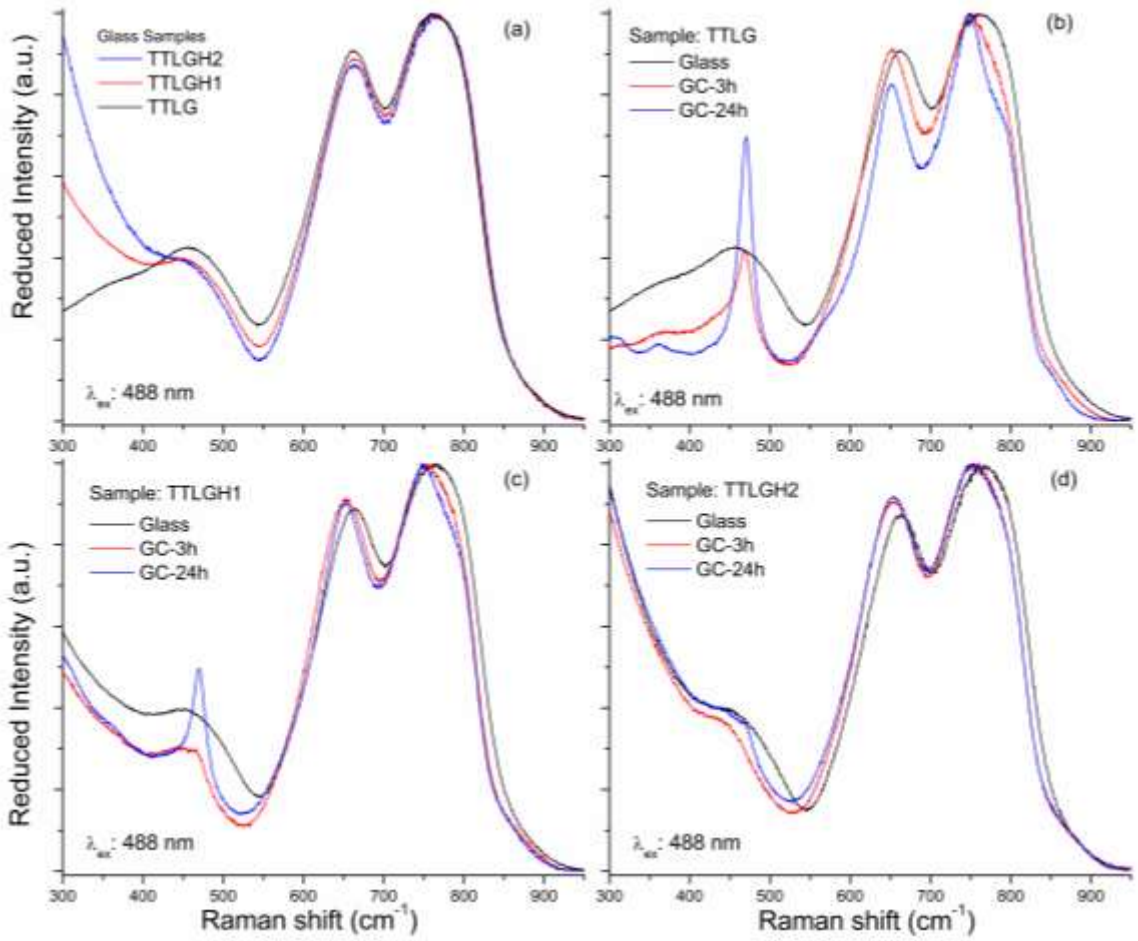

Figure S-V: Reduced and normalized Raman spectra excited at 488 nm, of (a) TTLG, TTLGH1, and TTLGH2 glass; glass and glass-ceramics of (b) TTLG, (c) TTLGH1, and (d) TTLGH2 sample.

respectively. However, to justify the basis of Raman bands appeared 200 – 450 cm^{-1} range, Raman spectra has been recorded under 488 nm Ar^{+} laser excitation and depicted in the Supplementary Information S-V (a-d). Figure S-V (a) reveals the Raman spectra of glass sample. This has demonstrated clearly that beyond 400 cm^{-1} of Raman shift, the Ho_2O_3-modified glass

samples have continuous increase of Raman scattering intensity. However, TTLG glass has

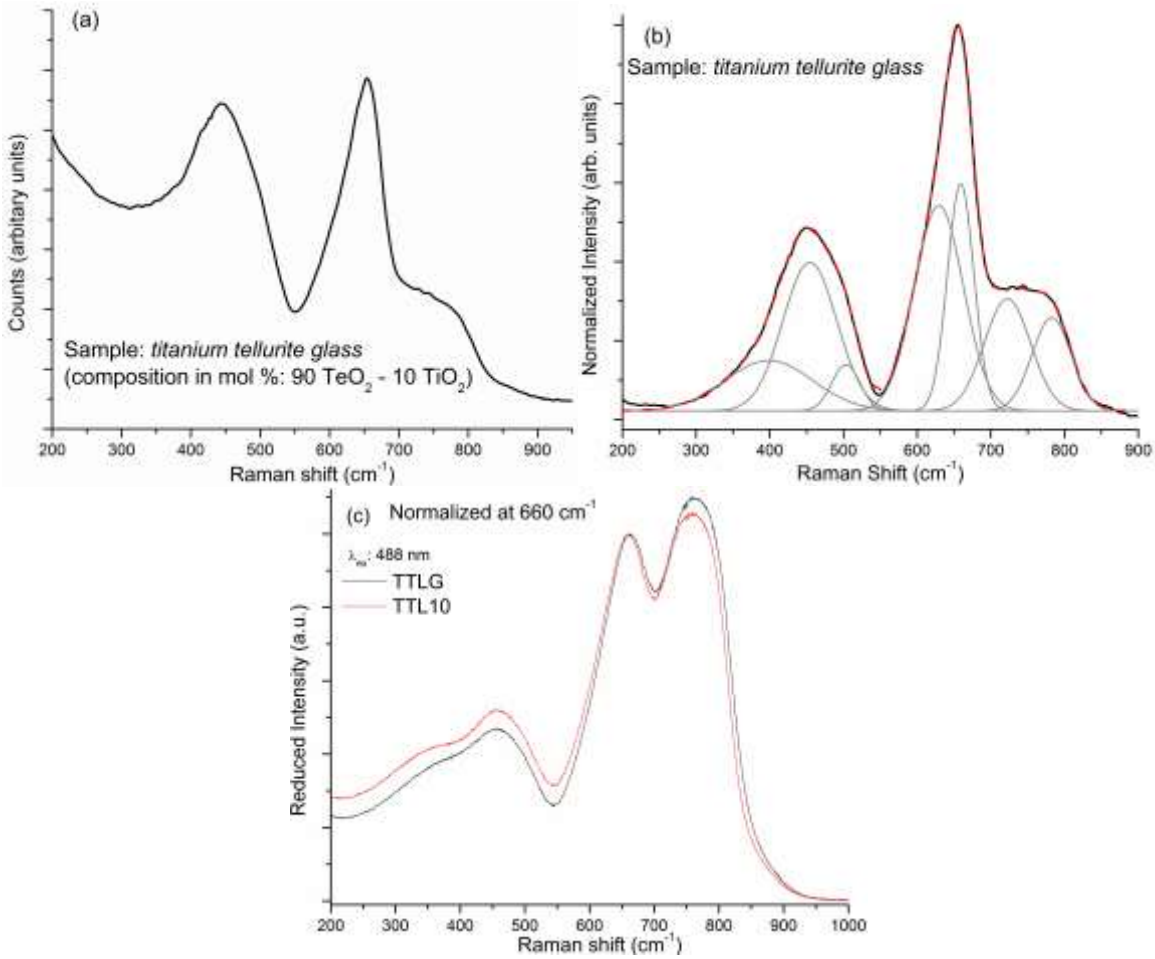

Figure S-VI: (a) measured Raman spectra of *titanium tellurite glass* (90 TeO_2 – 10 TiO_2), (b) deconvoluted and Gauss line fitted Raman spectra of baseline corrected *titanium tellurite glass,* and (c) reduced and normalized Raman spectra of TTLG and TTL10 glass.

shown steady decrease of scattering intensity beyond 400 cm^{-1} range. This confirms that the bands appeared in 200 – 450 cm^{-1} range is due to the luminescence from Ho^{3+}. Figures S-V (b-d) has revealed the Raman spectra of TTLG, TTLGH1, and TTLGH2 respectively with respective glass-ceramics. Significantly, for TTLG-based GCs sharp band appeared at 470 cm^{-1}. However, the increase of Ho_2O_3 content has reduced sharpness of Raman bands in GCs.

The partial fractions of area under every deconvoluted band have been presented in S-VII. To comprehend the local structure of *titanium tellurite glass* (90 TeO_2 – 10 TiO_2), the measured Raman spectrum has been depicted in the Supplementary information S-V (a). The baseline corrected and modified Raman spectrum of *titanium tellurite glass* has been deconvoluted by Gaussian line fitted and depicted in the Supplementary information S-V (b).

S6. Evaluation of average coordination number ($n_{Te\text{-}O}$)

On the basis of the partial area under the deconvoluted Gaussian line profiles, average coordination number ($n_{Te\text{-}O}$) for present series of glass samples were evaluated. Supplementary information S-V has been presenting the partial area under the Gaussian band. The Raman spectra in the range of 250 – 950 cm^{-1} have been considered for the present study, which is considered to be in two regions as (a) 250 – 550 cm^{-1} and (b) 550 – 950 cm^{-1}. The average coordination number (i.e. $n_{Te\text{-}O}$) has been estimated from the partial area under the 550 – 950 cm^{-}

Table SI-I: The deconvoluted partial area under the Raman spectra for each Gaussian band described as A_i (*i*: 1, 2, 3, 4, and 5), in the parenthesis peak position of decomposed Gaussian bands are presented in cm^{-1} and average coordination number ($n_{Te\text{-}O}$).

Sample	A_1 (%) ν (cm^{-1})	A_2 (%) ν (cm^{-1})	A_3 (%) ν (cm^{-1})	A_4 (%) ν (cm^{-1})	$n_{Te\text{-}O}$
titanium tellurite glass	26.12 (629)	15.57 (659)	13.41 (722)	3.47 (783)	3.65
TTLG	1.91 (586)	29.04 (661)	11.23 (738)	20.53 (791)	3.49
TTLGH1	1.82 (593)	29.50 (662)	11.39 (736)	26.44 (790)	3.45
TTLGH2	1.31 (591)	24.73 (662)	7.91 (735)	22.95 (790)	3.46

^{1} region.[3] The line profiles A_1 and A_2 have been associated to the TeO_4 structural units while, A_3 and A_4 have been related with TeO_{3+1} and TeO_3 structural units. Therefore, the average coordination number (i.e. $n_{Te\text{-}O}$) associated with present series of glass has been given as the weighted average of the partial area under the Gaussian line profiles.[4]

$$n_{Te-O} = \frac{3\times(A_4 + A_3) + 4\times(A_2 + A_1)}{(A_2 + A_3 + A_4 + A_1)} \qquad \text{(S-1)}$$

In case of *titanium tellurite* glass, with the systematic inclusion of lanthanides in the network the $n_{Te\text{-}O}$ has reduced steadily, which clearly reveal the formation of TeO_{3+1} and TeO_3

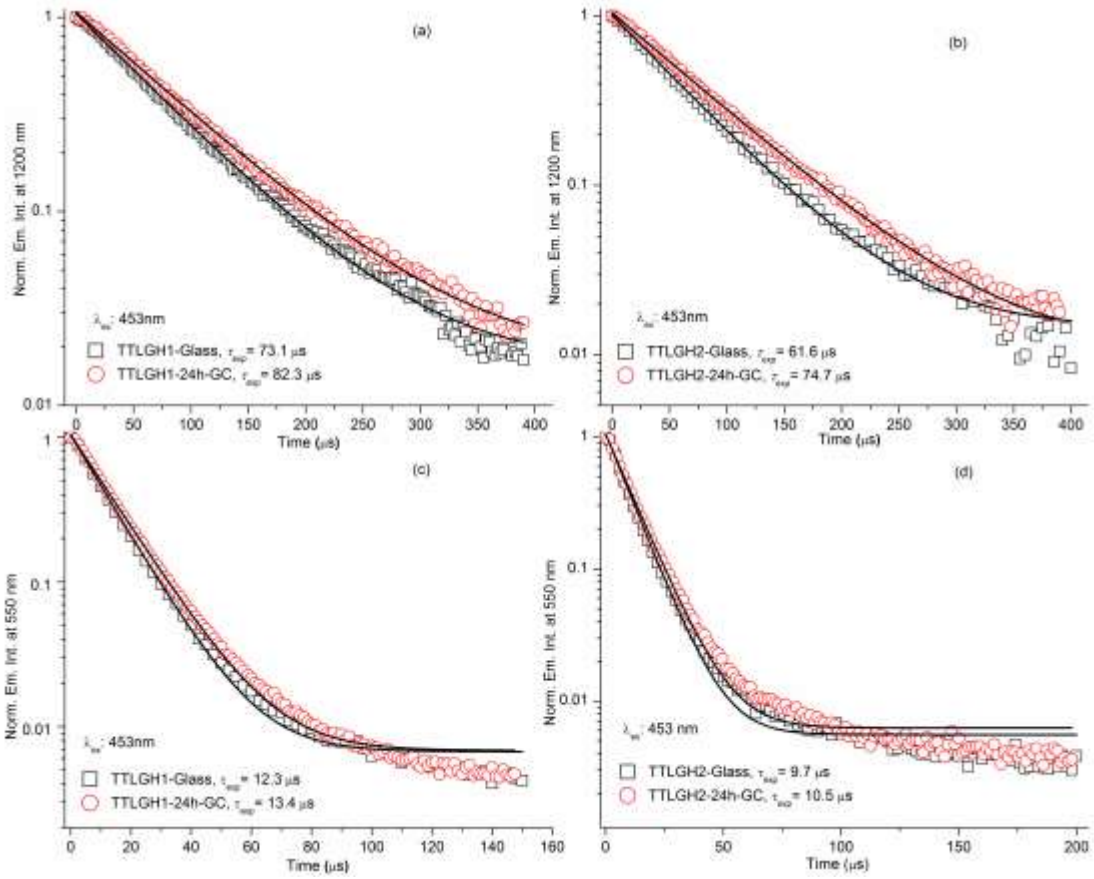

Figure S-VIII: Fluorescence decay curves at 1200 nm of (a) TTLGH1 and (b) TTLGH2 based glass and glass-ceramics as well as 550 nm of (c) TTLGH1 and (d) TTLGH2 based glass and glass-ceramics under 453 nm excitation.

units over TeO_4. Further analysis of Raman spectra of present series of glass have been discussed in the main text of the manuscript.

7. Fluorescence decay curves of Ho^{3+}: $^5S_2 \rightarrow {}^5I_8$ and $^5I_6 \rightarrow {}^5I_8$ transition

The fluorescence decay curves associated to Ho^{3+}: $^5S_2 \rightarrow {}^5I_8$ (550 nm) and Ho^{3+}: $^5I_6 \rightarrow {}^5I_8$ (1194 nm) have been depicted in S-VII. For Ho^{3+}: $^5S_2 \rightarrow {}^5I_8$ and Ho^{3+}: $^5I_6 \rightarrow {}^5I_8$ transitions the enhanced fluorescence lifetime have been realized for glass-ceramics compare to its glass counterpart. This confirms the enhanced fluorescence lifetime for transparent glass-ceramics for which, the low phonon crystal-field effect of transparent glass-ceramics can be attributed. Furthermore, the measured fluorescence lifetime has been decreased from TTLGH1 to TTLGH2 sample. The steady decrease in fluorescence lifetime from 1 mol% to 2 mol% Ho_2O_3 doped TTLG glass is implying the occurrence of concentration quenching effect.

References:

[1] G. Gupta, S. Balaji, K. Biswas, A. Kalyandurg, *Journal of the American Ceramic Society* **2018**, DOI: 10.1111/jace.15558.

[2] S. Chenu, E. Véron, C. Genevois, G. Matzen, T. Cardinal, A. Etienne, D. Massiot, M. Allix, *Advanced Optical Materials* **2014**, *2*, 364.

[3] E. R. Barney, A. C. Hannon, D. Holland, N. Umesaki, M. Tatsumisago, R. G. Orman, S. Feller, *The Journal of Physical Chemistry Letters* **2013**, *4*, 2312.

[4] A. G. Kalampounias, S. Boghosian, *Vibrational Spectroscopy* **2012**, *59*, 18.